

Abstract

Wood is the most important carrier of solar / renewable energy. The fuel characteristics with low ash and low sulfur content challenges coal, oil, and gas heating systems. The advantages of wood combustions include (i) a net reduction of greenhouse gases (CO₂-neutral emissions), (ii) detached from global marketing prices as wood production is predominantly associated to local dealers, and (iii) wood is a renewable energy source that can be harvested from one's backyard so to speak.

Modern heating systems such as the LogWIN-series of Windhager Zentralheizung Technik in Seekirchen Austria, are efficient and environmentally more sustainable than fossil fuel combustion. Hence, it was the aim of this study to investigate the particle emissions originating from wood-combustion during various modes of operation. The emitted particle inventory of a LogWIN 30kW solid fuel, wood heating systems was monitored during the start-up-, continuous phase and burnout-phase. The furnace is characterized by a discontinuous charging of roughly 50 cm long logs into the combustion chamber.

Introduction

Upon loading the feeder with beech-logs, the furnace was booted according to a strict protocol for either automatic or manual start-up routine.

Table 1: Technical data of the LogWIN burner

furnace design: water cooled heat exchanger at a nominal pressure [bar]	3
combustion capacity [kW]	32.5
nom.thermal output [kW]	13-29.9
filling chamber volume [L]	176
combustion cycle per load [h]	4-14*
exhaust mass flow-rate at nominal load [gs]	17.4
exhaust gas temp. at nom. load [°C]	143
furnace efficiency [%]	92
weight of furnace [kg]	463

* duration of a full combustion cycle depends on wood density, i.e. type of wood used. Dry wood has a typical calorific value of around 15.3 MJ/kg (Strehler, 2000).

Results

The furnace's particle mass inventory measured in a previous campaign in normal combustion mode emits slightly less particles than a state-of-the-art pellet burner (Oberberger et al., 2007). The overall particle mass measured in therein was found to range between 3-10 mg/m³ (full vs. partial load). However, Wiesner & Gaeogauf (2000) state that 95% of the particle emissions are found below the 400nm range. Thus, from an inhalation point of view, particle number concentration is more interesting. These were found to range from 4-5 and 6-7·10⁶ particles/cm³ (partial load of 15 kW vs. nominal load of 30kW) with a stable average aerosol diameter around 70 nm.

Aerosol characteristics during the start-up phase of the LogWIN-furnace differ somewhat, in that peak concentrations can reach 10-11·10⁶ particles/cm³ with an average aerosol diameter around 400 nm (i.e. visible smoke formation).

Figure 3 displays the particle distribution for both the start-up and the continuous combustion mode measured at the exhaust outlet some 90 cm downstream the chimney. The continuous combustion mode is characterized by a drastic particle-size shift from a coarse range around 300 nm to a finer range of about 70 nm.

During this continuous combustion mode, the generated aerosol was again monitored at end-of-stack (at roof-top, approximately 12m downstream the exhaust outlet).

The results of the inhalation and lung-deposition probabilities of this slightly altered end-of-stack-aerosol were modelled by the stochastic lung deposition model IDEAL, are shown in Fig. 4. According to the various HGFs (Hygroscopic Growth Factor, Ashgarian, 2004) - with HGFx1/x2/x5 corresponding to no/double and 5-fold increase of the original particle diameter - the obtained deposition of hydrophilic inorganic aerosols varies widely and covers a range of 14-25% (see legend in Fig.4). Yet, any of the three settings reveal distinct deposition peaks beyond the 15th generation, which belong to the pulmonary or alveolar region (Yeh & Schum, 1980). Such alveolar deposition is common for combustion aerosols. However, it should be noted that inhalation depends on the distance from the source and meso-climatic factors. Thus the values given at the right ordinate of Fig. 4 are maximal values when exposed directly to the stack plume. While any applicable dilution factor lowers this concentration maximum, it does not drastically alter the deposition of the distribution probability (is dependent on aerosol-aging effects).

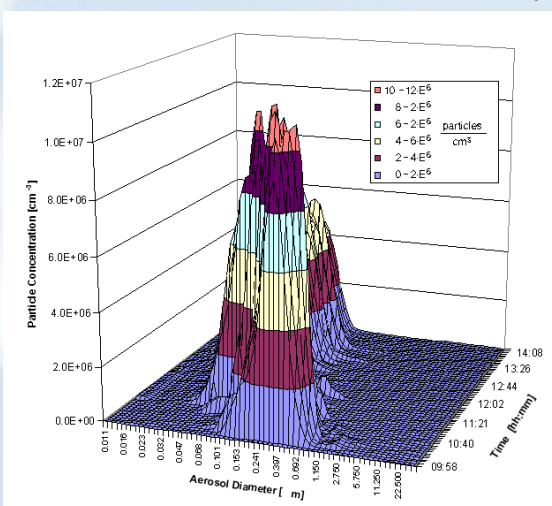


Fig. 3: Time-resolved aerosol distribution during start-up and normal combustion mode, measured 90 cm downstream the exhaust outlet of the furnace.

Conclusion

Although combustion of renewable energy sources such as wood has the potential to drastically reduce dependence and consumption of unsustainable energy sources, the aerosol load generated in such furnaces is still considerably high. Since it is known that alveolar deposition is associated with increased cardio-circulatory problems (Donaldson et al., 1988), treating the exhaust aerosols with an additional water nebulizer could significantly reduce the nano-aerosol fraction. In addition, such an additional treatment unit could further increase the energy efficiency of the entire unit by extracting remnant thermal energy from the exhaust gas stream. A similar cleaning effect has been shown by Kwasny et al. (2008), where a significant reduction in nano-particle concentration was observed. Electrostatic particle-precipitation should be another option in order to achieve even better cleansing result (Rengasamy et al., 2009).

References

- Ashgarian B. (2004). A model of hygroscopic particles in the human lung. *Aerosol Science and Technology*, 38: 938-947.
- Brunner T., Bärthaler G., Oberberger I. (2006). Fine particulate emissions from state-of-the-art small-scale Austrian pellet furnaces - characterisation, formation and possibilities of reduction. *BioEnergySystems*. available online (<http://www.bios-bioenergy.at/de/downloads-publikationen/pellets.html>)
- Donaldson, K., Li, X. Y., MacNee, W. (1988). Ultrafine (nanometre) particle mediated lung injury. *Journal of Aerosol Science*, 29: 553-560.
- Hofmann, W. & Koblinger, L. (1990). Monte Carlo modeling of aerosol deposition in human lungs. Part II: Deposition fractions and their sensitivity to parameter variations. *Journal of Aerosol Science*, 21: 675-688.
- Koblinger L. & Hofmann, W. (1990). Monte Carlo modeling of aerosol deposition in human lungs. Part I: Simulation of particle transport in a stochastic lung structure. *Journal of Aerosol Science*, 21: 661-674.
- Kwasny F., Madl P., Hofmann W. (2008). Effects of salt-aerosols from a gradierwerk on inhalation therapy and ambient air. *Berichte der Naturwissenschaftlich-Medizinischen Vereinigung in Salzburg*, Band 15: 99-108.
- Oberberger I., Brunner T., Bärthaler G. (2007). Fine particulate emissions from modern austrian small-scale biomass combustion plants. *Proceedings of the 15th European Biomass Conference & Exhibition*, Berlin. *ETA-Renewable Energies* (Ed.): 1546-1557.
- Rengasamy S., Eimer B.C., Shaffer R.E. (2009). Comparison of nanoparticle filtration performance of NIOSH-approved and CE-marked particulate filtering facepiece respirators. *Annals of Occupational Hygiene*, 53: 117-128.
- Strehler, A. (2000). Technologies of wood combustion. *Ecological Engineering*, Volume 16, Supplement 1: 25-40.
- Wieser U. & Gaeogauf C.K. (2000). Nanoparticle Emissions of Wood Combustion Processes. 1st World Conf. and Exhib. on biomass for Energy and Industry, Sevilla.
- Yeh, H. C. & Schum, G. M. (1980). Models of human lung airways and their application to inhaled particle deposition. *Bull. Math. Biol.* 42: 461-480.

Methods

The aerosol inventory was sampled 90 cm downstream the exhaust fume with a wide-range aerosol monitor consisting of an SMPS and an OPC operated in tandem mode. Since dry wood still contains up to 15% water (Strehler, 2000), a condensation trap was placed in-between the sample outlet and the measurement devices. Due to the extremely high aerosol concentrations during the start-up procedure, both instruments have been provided with a 1:100 dilution system.

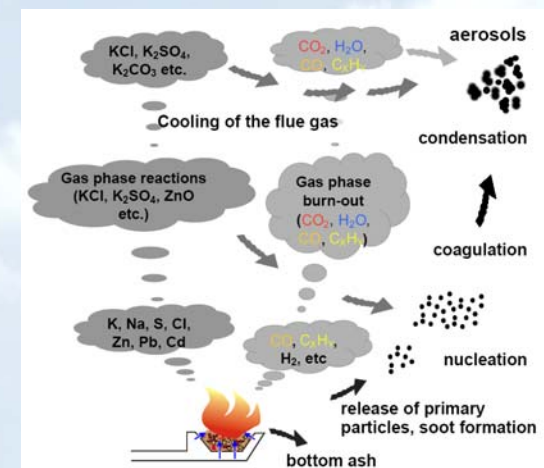


Fig. 2: Aerosol formation during biomass combustion (Brunner et al., 2006)

End-of-stack measurements were conducted in order to model the fate of inhaled aerosols once released into the environment. The data obtained from these measurements were then input into a stochastic lung model IDEAL originally developed by Koblinger & Hofmann (1990) and Hofmann & Koblinger (1990) to investigate the fate of inhaled particles. In this model, the geometry of the airways along the path of an inhaled particle is selected randomly, whereas deposition probabilities are computed by deterministic formulae.

Aerosol Formation

Depending on the flow conditions, coarse fly ash particles are partly precipitated in the furnace and the boiler (see Fig.1 & 2). The particles remaining in the flue gas leave the boiler as coarse fly ash emissions and range from a few μm up to 200 μm in diameter (Oberberger et al., 2007). Yet, from an inhalation point of view, the coarse fraction is insignificant in numerical numbers when compared to the finest fraction in the nanometer size range. This second type of aerosol emissions formed during biomass combustion can be divided into inorganic and organic aerosols. Fig. 2 shows a simplified scheme of the most relevant processes involved - for in-depth details we refer to Oberberger et al. (2007). At the boiler outlet, the aerosol fraction usually shows a quasi mono-disperse, log-normal particle size distribution. Due to the huge temperature gradient between the site of combustion and at the tailpipe end of the stack, nano-aerosols grow by coagulation processes.

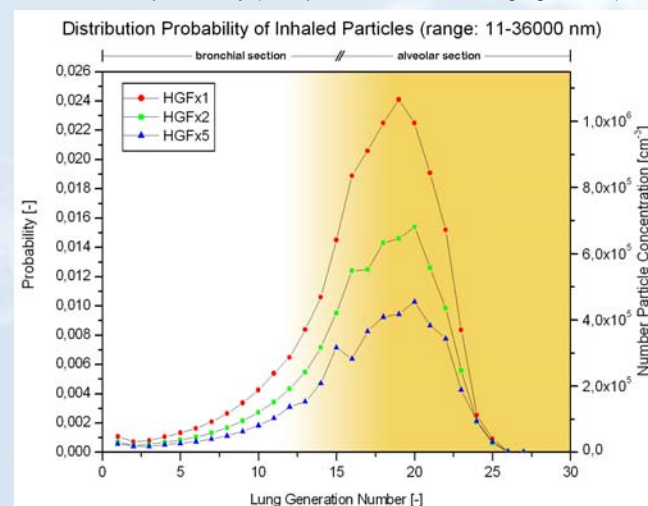


Fig. 4: Modelled deposition pattern of the end-of-stack aerosol, using the Monte Carlo code IDEAL. Plotted are three individual simulations for various Hygroscopic Growth Factors (HGF).